DOI: 10.1111/eci.12731

ORIGINAL ARTICLE

Paraoxonase-1 activity is related to *Trichinella spiralis*-induced hepatitis in rats

Ayman Samir Farid[*], Eman Mohamed Fath[†], Shogo Mido[†], Nariaki Nonaka[†,‡] and Yoichiro Horii[†,‡]

[*]Department of Clinical Pathology, Faculty of Veterinary Medicine, Benha University, Moshtohor, Toukh, Qalyubia, Egypt, [†]Laboratory of Veterinary Parasitic Diseases, Interdisciplinary Graduate School of Medicine and Veterinary Medicine, University of Miyazaki, Miyazaki, Japan, [‡]Center for Animal Disease Control, University of Miyazaki, Miyazaki, Japan

ABSTRACT

Background Little is known about the potential adverse effects of a chronic zoonotic nematode *Trichinella spiralis* infection on hepatic inflammation and its relationship to paraoxonase (PON)-1 and butyrylcholinesterase (BuChE) activities. Therefore, we aimed to examine the effects of *T. spiralis* infection on hepatic synthesis of PON1.

Methods Wistar rats were infected with 2500 first-stage larvae (L1) of *T. spiralis*, and serum PON1 and BuChE activities were evaluated. Hepatic expression levels of PON1, BuChE and various cytokines and chemokines [interleukin (IL)-1, IL-4, IL-6, IL-10, tumour necrosis factor (TNF)-α, monocyte chemoattractant protein (MCP)-1, macrophage inflammatory protein (MIP)-1α, and transforming growth factor (TGF)-β1] were evaluated for up to 9 weeks post-infection (p.i.). The effect of these changes on the degree of hepatic apoptosis was also investigated.

Results *Trichinella spiralis* infection in rats induced significant decreases in serum PON1 activities from day 2 until week 7 p.i. and BuChE activity starting from day 4 until 2 weeks p.i. Moreover, *T. spiralis* infection increased serum pro-inflammatory cytokines IL-1, IL-6 and TNF-α as well as chemokines MCP-1, MIP-1α and TGF-β1 during the enteral phase of the parasite life cycle. The anti-inflammatory cytokines IL-4 and IL-10 showed significant increases during the enteral phase for the former and the muscle phase for the latter. These were associated with hepatic inflammation and apoptosis. These events typically decreased hepatic PON1 and BuChE mRNA expression.

Conclusions Immune responses mounted against *T. spiralis* infection in rats were associated with hepatic inflammation and a subsequent decrease in serum PON1 and BuChE activities.

Keywords apoptosis, butyrylcholinesterase, hepatitis, paraoxonase, *Trichinella spiralis*.

Eur J Clin Invest 2017; 47 (3): 250–261

Introduction

The liver performs many crucial metabolic activities, but it also functions in immune defence [1]. The liver filters out potentially immunogenic material in portal blood before entering the systemic circulation. Against continuous exposures of harmless and harmful substances, the liver discriminates them effectively and generates appropriate immune responses [2,3]. Failure can alter immune response and often resulting in tissue damage [4]. Liver diseases are inflammatory processes accompanied by increasing in cytokines and chemokines. At the same time, in response to infection, tissue damage or acute inflammation, the host undergoes a series of biochemical and physiological changes termed as the acute-phase response. This is an innate immune response which plays a critical role in altering tissue damage. The synthesis of proteins in the liver in relation to coagulation, lipid metabolism and the complement system are often altered by the response [5].

Paraoxonase-1 (PON1) is a high-density lipoprotein (HDL)-associated enzyme known as a free radical scavenging system related to the acute phase response [6]. PON1 is synthesized primarily in the liver and secreted into plasma and its natural physiological function is metabolism of toxic oxidized lipids of both low-density lipoprotein (LDL) and HDL particles [7]. PON1 exerts anti-atherogenic/anti-inflammatory effects through the hydrolysis of lipid peroxides and retards LDL oxidation. In addition, it inhibits the oxidation of not only LDL but also HDL [8]. Paraoxonase exerts a continuous reverse cholesterol transport from the arterial wall to the liver for excretion [9]. This situation retards the development of

macrophage foam cell formation and atherosclerosis [10,11]. The concentration and/or the activity of PON1 can be modified by various infections [12].

Butyrylcholinesterase (BuChE) (pseudocholinesterase or plasma ChE) is produced by the liver and is present in serum, the pancreas and the central nervous system. Although the functions of this enzyme are unknown, studies in humans and dogs have related BuChE to lipid metabolism and its activity is increased during lipid mobilization [13,14]. The pharmacological and toxicological importance of BuChE is evidenced by its ability to hydrolyze ester-containing compounds such as cocaine and succinylcholine as well as acting as a scavenger against neurotoxic organophosphates [15].

We have previously described the effects of nematode infections on serum PON1 activities in laboratory animals [16–19]. Mido *et al.* (2012) [16] reported that *T. spiralis* infection in rats induced a significant reduction in serum PON1 activities associated with status of oxidative stress as well as an atherogenic lipid profile. *T. spiralis* infection is typified by intestinal and muscular phases, corresponding to two distinct periods in the parasite's life cycle in the host. Each of these phases may influence the immune response of the host uniquely [20]. The host immune response during the intestinal phase of *T. spiralis* infection is characterized by mixed Th1/Th2 responses with the initial predominance of the Th1 and the subsequent predominance of the Th2. Th2-type responses involving interleukin (IL)-4, IL-10 and IL-13 are essential in the expulsion of gastrointestinal adult *T. spiralis*. Anti-inflammatory effects of IL-10 limit the immune response against the early stages of muscle larvae of *T. spiralis*, but sustained control of inflammation during chronic muscle infection does not depend on it and there is a shift to a Th2 response [21]. Nonetheless, our current knowledge with respect to the mechanisms responsible for regulating PON1 activity during *T. spiralis* is incomplete.

Considering the complex known and unknown cellular and molecular mechanisms involved in the pathophysiology of hepatic PON1 and BuChE synthesis, we aimed to explore the effects of *T. spiralis* infection on hepatic PON1 and inflammatory marker expression.

Methods

Experimental animals

Fourteen-week old male Wistar rats (375–390 g) were obtained from Charles River Japan, Inc., Yokohama, Japan. All animals were housed in clean cages and given a standard diet and clean water *ad libitum*. Their environment was controlled in terms of light (12-h light-dark cycle starting at 8:00 AM) and room temperature (23 ± 3 °C). The study performed with approval from the institutional review board for animal experiments of the University of Miyazaki (Approval No. 2014-014-2), in compliance with the laws of Japan 'Act on Welfare and Management of Animals'. All animal procedures were conducted in BSL2 room.

Parasitological techniques

To infect the experimental rats, *T. spiralis* (code ISS3) first-stage larvae (L1) were recovered from the muscles of mice which had been infected for > 4 weeks as described previously by Crum *et al.* (1977) [22]. In brief, donor mice were euthanized by cervical dislocation and skinned and eviscerated carcasses were minced in a meat grinder and digested for 1–2 h at 37 °C in distilled water (10 mL/g) containing 1% [weight/volume (w/v)] pepsin (Sigma Chemical Co., St. Louis, MO, USA) and 1% (v/v) HCl. Larvae were isolated by passing the digestion mixture through a 200-mesh screen and washed several times with 0·85% NaCl. Animals randomized to the *T. spiralis* group were given 2500 L1 by oral gavage. Muscle stage larvae were counted under a microscope following digestion of the whole carcass of infected rats as previously described [22] and removal of the pepsin–hydrochloride solution. Intestinal *T. spiralis* stages were obtained from the intestines of infected rats from 2 days p.i. until the end of the experiment using the Baermann technique.

Serum PON1 activity

Serum PON1 activity was assayed using three synthetic substrates: paraoxon (diethyl-*p*-nitrophenyl phosphate; Sigma Chemical Co.), phenyl acetate (Nacalai Tesque, Inc, Kyoto, Japan) and dihydrocoumarin (Sigma Chemical Co.) [23]. All activities were measured at 25 °C.

Analysis of mRNA expression of hepatic PON1, IL-1, Il-4, IL-6, IL-10, TNF-α, MCP-1, MIP-1α, BuChE and TGF-β1 genes using real-time PCR

To better understand the effect of *T. spiralis* infection on hepatic inflammation and its relationship with PON synthesis, expression of hepatic PON1 as well as various cytokines, chemokines and enzymes was analysed by real-time PCR using sense and anti-sense primers throughout the experiment as previously described [17] using the following primers sets: PON1 (GenBank ID: NM_032077.1), sense (5′-AAG TAT GTC TAT ATC GCT GAA TTG C-3′) and anti-sense (5′-CAC AGG ATC CAC AGA GAT GTT ATC-3′); BuChE (GenBank ID: NM_022942.1), sense (5′-AGA ATG GAT GGG AGT AAT GCA TGG-3′) and anti-sense (5′-GCT ATT GCC CTG AGT CCC ATT GG-3′); IL-1β (GenBank ID: M98820.1), sense (5′-CAC CTC TCA AGC AGA GCA CAG-3′) and anti-sense (5′-GGG TTC CAT GGT GAA GTC AAC-3′); IL-6 (NM_012589.2), sense (5′-TCC TAC CCC AAC TTC CAA TGC TC-3′) and anti-sense (5′-TTG GAT GGT CTT GGT CCT TAG CC-3′); TNF-α (GenBank ID: NM_012675.3), sense (5′-AAA TGG GCT CCC TCT CAT CAG TTC-3′) and anti-sense (5′-TCT GCT TGG TTT GCT ACG AC-3′); MCP-1 (GenBank ID: NM_031530.1),

sense (5′-ATG CAG TTA ATG CCC CAC TC-3′) and anti-sense (5′-TTC CTT ATT GGG GTC AGC AC-3′); MIP-1α (GenBank ID: NM_013025.2), sense (5′-CAT TCC TGC CAC CTG CAA AT-3′) and anti-sense (5′-CAA GTG AAG AGT CCC TGG ATG TG-3′); TGF-β1 (NM_021578.2), sense (5′-CGT GGA AAT CAA TGG GAT CAG-3′) and anti-sense (5′-CAG GAA GGG TCG GTT CAT GT-3′); IL-4 (GenBank ID: NM_031512.2), sense (5-CAG GGT GCT TCG CAA ATT TTA C-3′) and anti-sense (5′-ACCG AGA ACC CCA GAC TTG TT-3′); IL-10 (GenBank ID: L02926.1), sense (5′-AGA AGC TGA AGA CCC TCT GGA TAC-3′) and anti-sense (5′-GCT CCA CTG CCT TGC TTT TAT T-3′); and 18S rRNA (GenBank ID: NR_046237.1) as a housekeeping gene, sense (5′-GAG GTG AAA TTC TTG GAC CGG-3′) and anti-sense (5′-CGA ACC TCC GAC TTT CGT TCT-3′).

Thermal cycling and fluorescence detection were performed using a 7300 real-time PCR system (Applied Biosystems, Foster City, CA, USA).

Changes in gene expression were calculated from the obtained cycle threshold (C_t) values provided by real-time PCR instrumentation using the comparative CT method to a reference (housekeeping) gene (18S rRNA) [24].

Histopathological analysis

The right liver lobes were collected from control and *T. spiralis*-infected rats and were fixed in neutral buffered formalin (pH 7·2) (Nacalai Tesque Inc., Kyoto, Japan). Sections from each liver specimen were stained with hematoxylin and eosin (HE) and Congo red stains to examine tissue for inflammatory cell infiltration (lymphocytes, neutrophils and eosinophils), histopathological changes in liver cells and amyloid deposition.

Terminal deoxynucleotide transferase-mediated terminal uridine deoxynucleotidyl transferase nick end-labelling (TUNEL) assay

Apoptotic cells in liver sections were detected by terminal deoxynucleotide transferase-mediated TUNEL using the APO-BrdU-IHC TUNEL Assay Kit (APO002, AbD Serotec, UK), according to the manufacturer's protocol. Briefly, paraffin-embedded liver sections (5 μm) were layered onto glass slides, dewaxed in xylene and rehydrated through graded dilutions of ethanol. Sections were treated with freshly diluted proteinase K (20 μg/mL) for 15 min at room temperature. Equilibration buffer was applied directly to the liver sections followed by incubation with the TUNEL reaction mixture containing terminal deoxynucleotidyl transferase (TdT), digoxigenin nucleotide and unlabelled nucleotides for 1 h in a humidified chamber at 37 °C. Anti-digoxigenin conjugate was applied directly to the slides and sections were counter stained with propidium iodide (PI), mounted and apoptotic cells were then visualized and counted under a light microscope (Nikon Eclipse 80i, Melville, New York, NY). TUNEL-positive cells were counted under high-power magnification (400 ×) in a blinded fashion. On each slide, 10 fields were randomly selected. Apoptotic index was calculated according to the formula AI = (AC/AC + IC) × 100 (Apoptotic index: AI, Apoptotic cell number: AC, Intact cell number: IC) [25]. The control was established with the positive and negative cells provided in the kit following the same protocol as described above.

Experimental design

In all, 74 male Wistar rats were randomly allocated into two groups (4–6 animals per group): a control group and a *T. spiralis*-infected group. Blood for serum samples was collected from the jugular vein of all animals on days 0, 2 and 4, and weeks 1–7, and week 9 post-infection (p.i.).

Statistics

Statistical analysis was performed using the statistical software package SPSS for Windows (Version 16.0; SPSS Inc., Chicago, IL, USA). Student's *t*-test was used to determine significant differences between *T. spiralis*-infected groups and controls at each checkpoint. Results are expressed as mean ± standard error of the mean (SEM). $P < 0{\cdot}05$ were considered to be statistically significant.

Results

Monitoring of *T. spiralis* infection by recovery of intestinal phase and muscle phase

Infection with *T. spiralis* larvae was monitored as shown in Fig. 1a. After oral infection of male Wistar rats with 2500 L1 of *T. spiralis*, intestinal stages were counted from day 2 p.i. and gradually declined through days 4 and 7 reaching a minimum by weeks 2 and 3 p.i. before completely disappearing by 5 weeks p.i. On the other hand, muscle stage larvae were detectable by the digestion method in the body musculature at week 2 p.i and gradually increased during week 3, reaching a plateau from week 5 until week 9 p.i. Loss of body weight followed the course of *T. spiralis* infection in the rat. Significant body weight losses were detected from day 4 until 7 weeks after infection ($P < 0{\cdot}05$) (Fig. 1b).

Serum enzymatic activities

Comparison of the results obtained for the control rats with those infected with *T. spiralis* indicates the impact of infection on the enzymatic PON1 activity. The paraoxonase activity of PON1, measured with paraoxon as a substrate, was found to be significantly lower in the *T. spiralis*-infected group by 23, 32, 56, 47, 40, 46 and 22% ($P < 0{\cdot}05$) on days 2, 4 and 7, and weeks 2, 3, 5 and 7, respectively, compared to the control group (Fig. 2a). Relative to the control group, *T. spiralis*-infected rats showed significant decreases in lactonase activity of PON1, which was

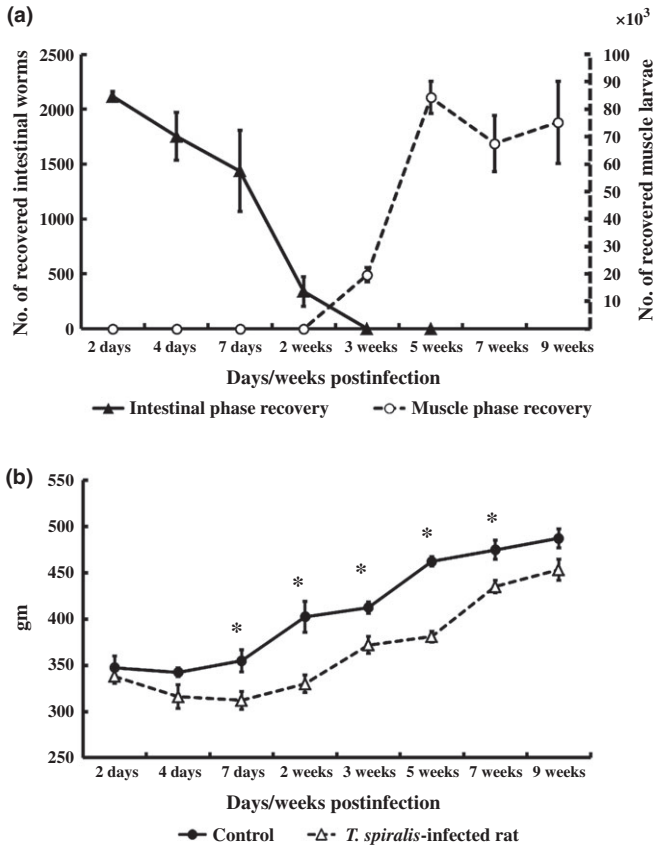

Figure 1 Number of intestinal phase worms and muscle stage larvae as well as body weight changes. Recovered intestinal phase worms and muscle stage larvae (a) and changes in bodyweight [Control vs. *T. spiralis* infected] (b) in male Wistar rats after infection with 2500 L1 of *T. spiralis*.*$P < 0{\cdot}05$ compared with control values. Bars represent means ± SEM ($n = 4$–6).

measured with dihydrocoumarin as a substrate, on days 2, 4 and 7, and weeks 2, 3, 5 and 7 by 17, 29, 54, 42, 33, 40 and 17%, respectively (Fig. 2b). Also, the arylesterase activity of PON1, measured with phenyl acetate as a substrate, was reduced significantly by 8, 18, 44, 25, 19 and 25% ($P < 0{\cdot}05$) on days 2, 4 and 7 and weeks 2, 3, 5 and 7, respectively, in comparison to the control group (Fig. 2c). The activity of another liver-synthesized enzyme, butyrylcholinesterase, showed significant ($P < 0{\cdot}05$) reductions by 20, 27, and 28% on days 4 and 7 and 2 weeks p.i., respectively (Fig. 2d).

Changes in hepatic PON1, BuChE, IL-1, IL-6, TNF-α, MCP-1, MIP-1α, TGF-β1, IL-4 and IL-10 mRNA expression following *T. spiralis* infection

Figure 3 shows the intensity of hepatic PON1, BuChE, IL-1, IL-6, TNF-α, MCP-1, MIP-1α, TGF-β1, IL-4 and IL-10 mRNA normalized to 18s rRNA in the *T. spiralis*-infected rats compared with control rats on days 2,4 and 7, and weeks 2, 3, 5, 7 and 9.

Infection with *T. spiralis* induced a significant ($P < 0{\cdot}05$) down-regulation in PON1 mRNA on days 4 (1·5-fold) and 7 (4·7-fold), as well as week 2 (4·5-fold) p.i. without significant changes from week 3 until week 9 p.i. BuChE mRNA expression in the liver of rats infected with *T. spiralis* was significantly down-regulated by 1·8, 2·2 and 2·8-folds on days 2, 4 and 7 p.i. (Fig 3a). At the same time, IL-1 showed a significant up-regulation (8-fold; $P < 0{\cdot}05$) on day 7 p.i. without significant changes at the other checkpoints. IL-6 mRNA expression in the hepatic tissue of *T. spiralis*-infected rats was significantly ($P < 0{\cdot}05$) increased on days 4 and 7 p.i. by 40 and 38 fold, respectively. The results showed that there is a significant increase ($P < 0{\cdot}05$; 6 fold) in hepatic TNF-α mRNA expression on day 7 p.i. (Fig. 3a). MCP-1 hepatic expression was significantly ($P < 0{\cdot}05$) up-regulated by 7, 9 and 5 folds on days 4 and 7 and week 2, respectively. MIP-1α mRNA hepatic expression was significantly increased by 2·5 and 11 folds on days 4 and 7 p.i., respectively. Also, hepatic TGF-β1 showed significant up-regulation by 2, 2·2, 3 and 2·8-folds on days 2, 4, 7 and 2 weeks p.i., respectively (Fig. 3b). Notably, IL-4 mRNA expression showed significant ($P < 0{\cdot}05$) up-regulation in hepatic tissue by 4, 382 and 2·5-folds on days 4 and 7, and 2 weeks p.i., respectively. Infection of rats with *T. spiralis* induced a significant ($P < 0{\cdot}05$) up-regulation of hepatic IL-10 expression at week 7 p.i. followed by a significant ($P < 0{\cdot}05$) down-regulation (3-fold) by week 9 p.i. (Fig. 3c).

Histopathological examination of hepatic tissue

To identify the correlation between changes in hepatic function manifested by reduced serum PON1 and BuChE activities and the hepatic innate immune response, we checked the liver sections stained with HE and Congo red. The examined sections showed inflammatory cell infiltrations (lymphocytes, neutrophils and eosinophils) especially around the portal vein and in the septa between hepatic lobules. These infiltrations were evident by day 2 through days 4 and 7 p.i. as well as at weeks 2, 3 and 5 p.i. Moreover, there was hepatic pyknosis on week 5 p.i. and hydropic degeneration in the hepatocytes at week 7 p.i. The liver tissues appeared to be normal by week 9 p.i (Fig. 4). Amyloid deposition was evident especially around blood vessels in the liver tissue on days 2, 4, 7 and week 2 p.i. as shown in Congo red stained sections (Fig. 5). Parallel to these histopathological changes in the liver tissue, there was a significant increase in apoptotic TUNEL-positive cells on days 4, 7 as well as weeks 2 and 3 p.i. (Fig. 6).

Discussion

Hepatic innate immune responses are involved and contribute to the systemic response to local inflammation, clearance of

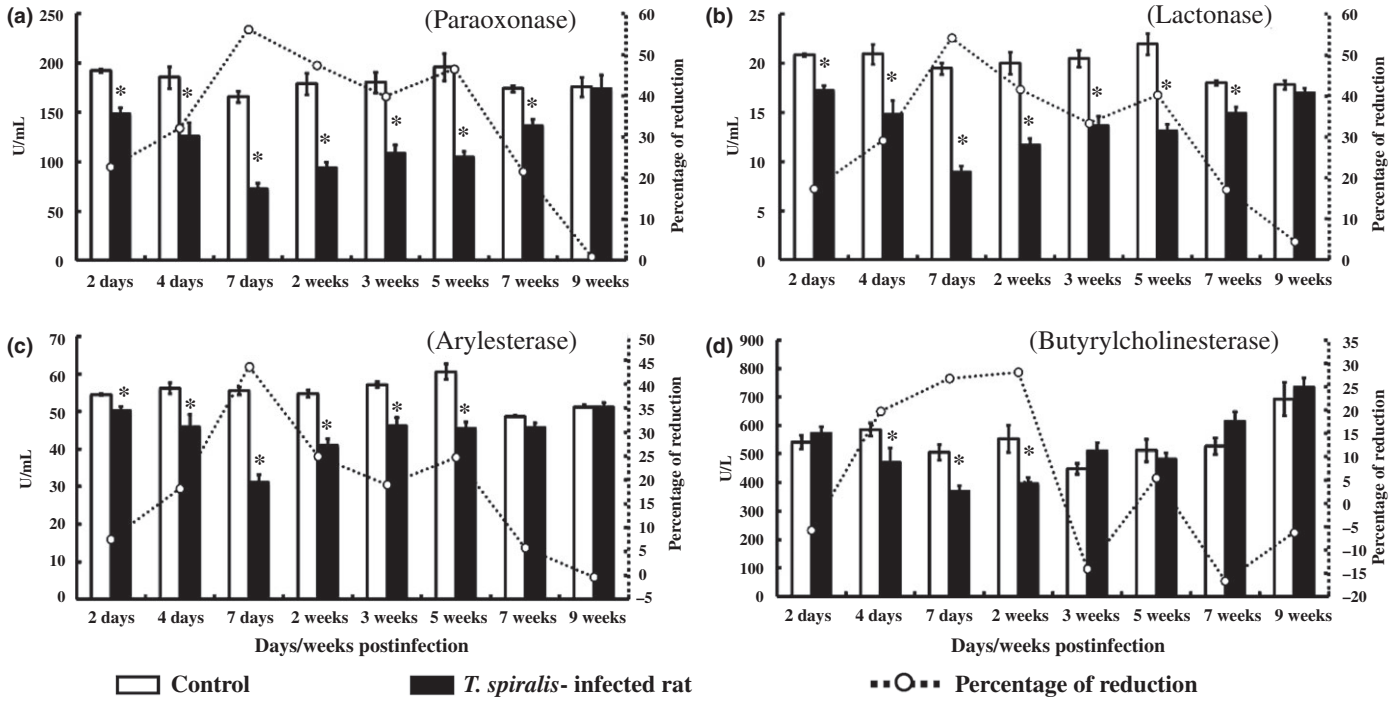

Figure 2 Effect of *T. spiralis* infection on serum PON1 and butyrylcholinesterase activities. Paraoxonase (a), lactonase (b), arylesterase (c) and butyrylcholinesterase (d) activities in male Wistar rats on days 2, 4 and 7 and weeks 2, 3, 5, 7 and 9 p.i. $*P < 0{\cdot}05$ compared with control values. Bars represent means ± SEM (n = 4–6).

particles and soluble molecules from the circulation, and killing of invading cells such as neoplastic cells [26]. In our previous work, we investigated the correlation between intestinal infection and liver functions and the immunological response.

We found that *T. spiralis* infection significantly decreased body weight starting from day 7 until week 7 p.i. This might have resulted from a decrease in food intake during *T. spiralis* infection as a result of an increase in cholecystokinin expressing enteroendocrine cells, under the control of IL-4 and IL-13 secreting $CD4^+$ T cells [27]. Cholecystokinin, in large part, induces its effects via a delay in gastric emptying [28].

Moreover, we found that *T. spiralis* infection significantly decreased serum PON1 and BuChE activities in Wistar rats. The observed reduction in serum PON1 (paraoxonase, lactonase and arylesterase) activity was similar to that reported previously [16]. In the current study, we expand on these results, and address the correlation between serum enzymatic activity and its hepatic synthesis as well as the association with hepatic inflammatory status. Our results showed a significant reduction in serum paraoxonase and lactonase activities from day 2 which continued until week 7 p.i. and up to week 5 p.i. for arylesterase activity. The reduction of serum PON1 covered both the intestinal and early muscle phases. On the other hand, the activity of BuChE was significantly reduced from day 4 until week 2 p.i. (only during intestinal phase).

Importantly, we found that serum PON1 activity is significantly decreased during the intestinal phase of *T. spiralis* infection in rats with a parallel decrease in liver mRNA (Fig. 3a). The reduction of PON1 activity in this model is proportional to degree of hepatic PON1 mRNA down-regulation during the enteral phase. Nonetheless, the observation is supported by evidence from previous studies consistent with the idea that serum PON1 activity is closely correlated with hepatic PON1 mRNA levels [6,29,30]. Similarly, the hepatic expression of BuChE mRNA is down-regulated during the intestinal phase. Liver inflammatory status associated with *T. spiralis* infection is one of the mechanisms responsible for hepatic PON1 and BuChE mRNA down-regulation during this infection in rats. This hepatic inflammation is evidenced by significant up-regulation of pro-inflammatory cytokines IL-1 (day 7 p.i.), IL-6 (days 4 and 7 p.i.) and TNF-α (day 7 p.i.). These results are supported by the results of Kumon *et al.* [31] who found that hepatic PON1 is down-regulated following treatment with TNF-α and IL-1. The role of pro-inflammatory cytokines in down-regulation of PON1 mRNA is thus primarily mediated by nuclear factor-κB (NF-κB) [32]. The same

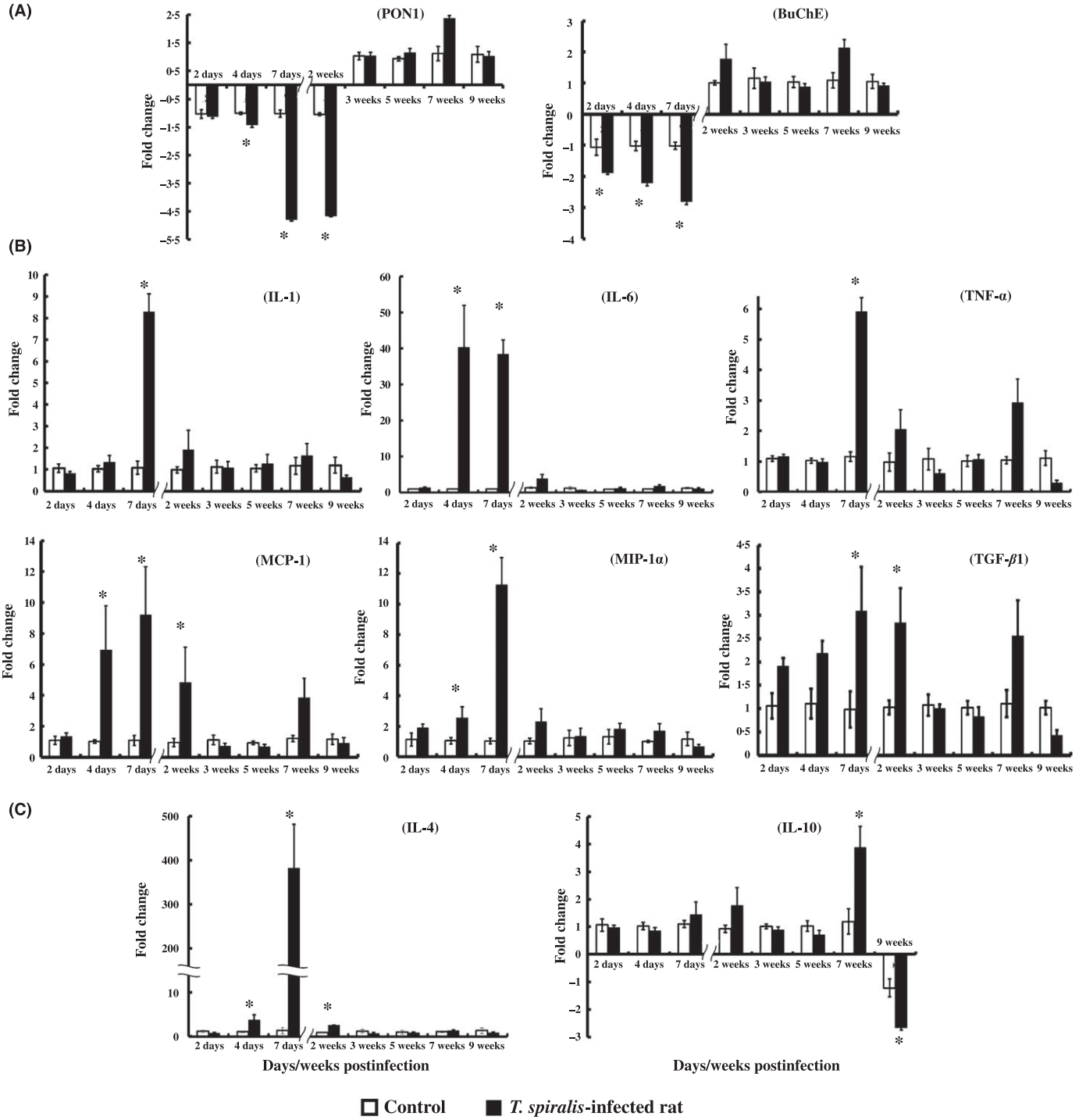

Figure 3 Messenger RNA expression of hepatic PON1, BuChE, IL-1, IL-6, TNF-α, MCP-1, MIP-1α, TGF-β1, IL-4 and IL-10 genes. Total RNA was prepared from hepatic tissues of rats infected with *T. spiralis* and controls on days 2, 4, and 7 and weeks 3, 5, 7 and 9 p.i. The expression levels were evaluated by real-time PCR. *$P < 0{\cdot}05$ compared with control values. Bars represent means ± SEM (n = 4–6).

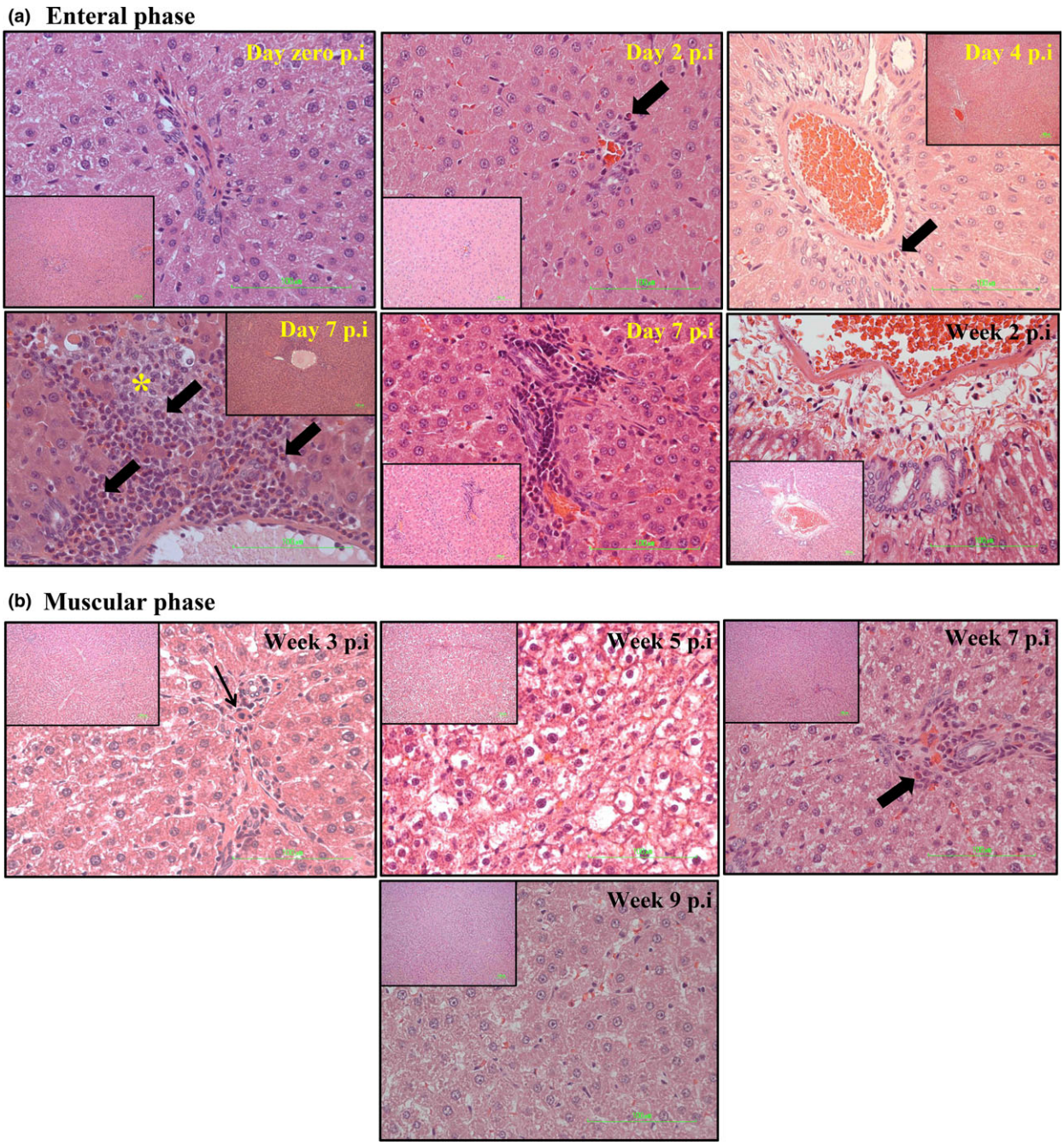

Figure 4 Histopathological examination of rat liver sections on different days following infection with 2500 L1 *T. spiralis*. Liver sections were deparaffinized, stained with hematoxylin–eosin (HE), and examined under light microscopy. Bold arrows indicate eosinophils, narrow arrows indicate plasma cells and yellow stars indicate accumulation of inflammatory cells (lymphocytes, neutrophils and eosinophils) on days 2, 4 and 7, and weeks 2, 3, 5,7 and 9, as well as control liver section with no abnormalities (day 0 p.i.). Scale bars, 100 μm (high-power field) and inset scale bars, 100 μm (low-power field).

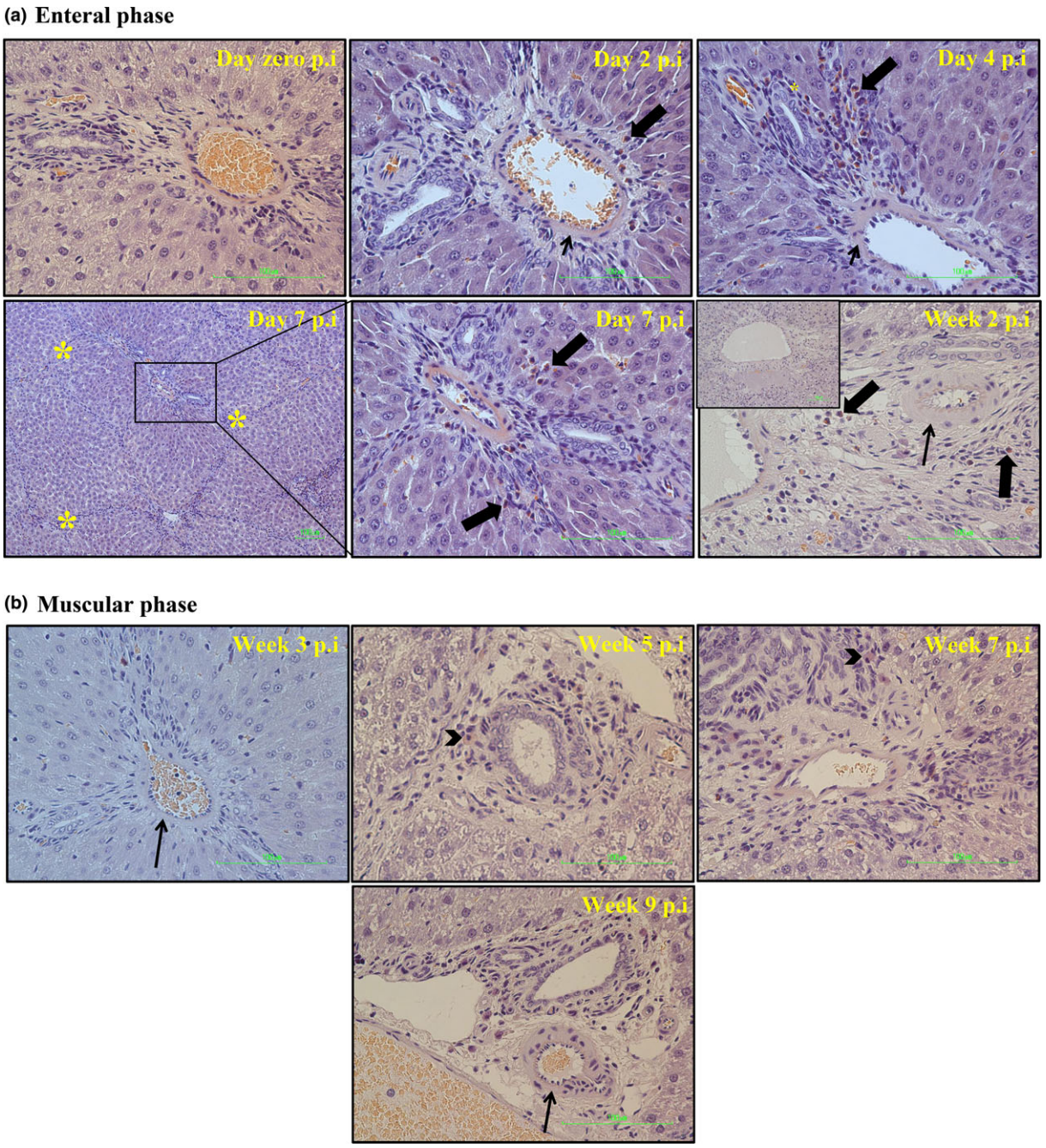

Figure 5 Congo red-stained sections of liver tissues of *T. spiralis*-infected rat on different days following infection with 2500 L1 *T. spiralis*. Liver sections were stained Congo red on different check points after *T. spiralis* infection. Bold arrows indicate eosinophils, narrow arrows indicate amyloid deposition, head arrows indicate plasma cells and yellow stars indicate accumulation of inflammatory cells (lymphocytes, neutrophils and eosinophil) on days 2, 4 and 7, and weeks 2, 3, 5, 7 and 9 as well as control liver section with no abnormalities (day 0 p.i.). Scale bars, 100 μm (high-power field) and inset scale bars, 100 μm (low-power field).

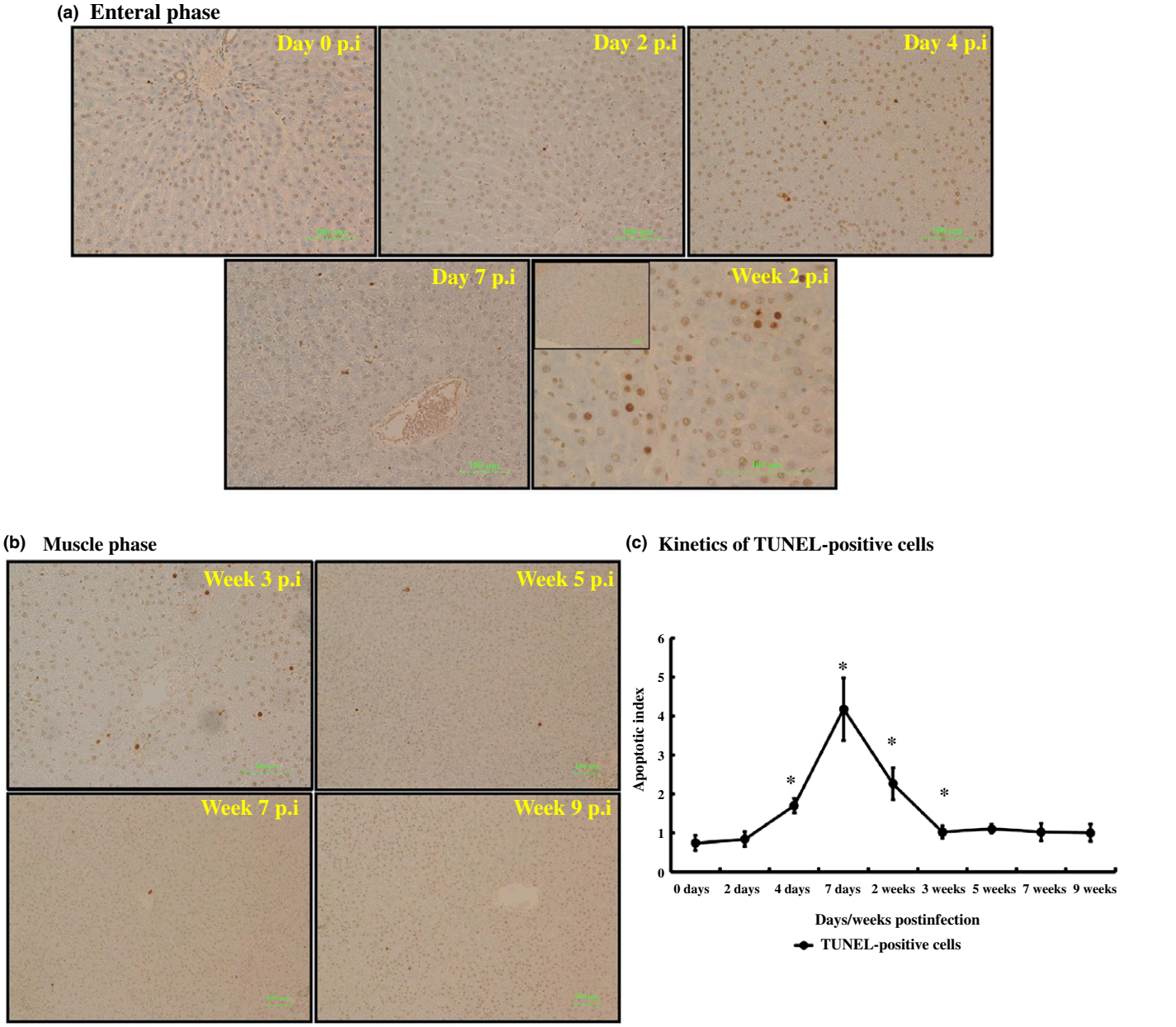

Figure 6 Apoptotic cell death in liver sections was detected using the TUNEL kit. TUNEL-positivity in liver specimens collected from *T. spiralis*-infected rats on days 0, 2, 4 and 7, and week 2 (a) and weeks 3, 5, 7 and 9 p.i. (b). Scale bars, 100 μm (high-power field) and inset scale bars, 100 μm (low-power field). (c) Bar graph of the numbers of TUNEL-positive cells per high-power field. *$P < 0{\cdot}05$ vs. control rat. Bars represent means ± SEM ($n = 4$).

mechanism of increased hepatic inflammatory cytokines (IL-1, IL-6 and TNF-α) down-regulates the expression of the BuChE gene function [33]. This finding is supported by our previous results that showed a reduction in serum BuChE activity 7 days after *Nippostrongylus brasiliensis* infection coinciding with the maximum inflammatory response against the infection [19].

It is interesting to note that the reduction of serum PON1 activities started (day 2 p.i.) before the down-regulation of its hepatic synthesis (day 4 p.i.), while the reduction in serum BuChE activity was noted after (day 4 p.i.) the down-regulation of its hepatic synthesis (day 2 p.i.). The reason for this might be due to increased PON1 enzyme degradation and/or structural

alterations of its protein molecules caused by free radical action [16,34,35], in addition to the differences in serum half-lives for both enzymes. The serum half-life of PON1 is ~ 6 h [36], while in the case of serum BuChE it is 9–11 days [37].

In our study, we found significant over-expression of pro-inflammatory mediators (IL-1, IL-6, TNF-α and MIP-1α). IL-1 is a potent inflammatory cytokine mainly produced by macrophages [38] and was significantly over-expressed on day 7 p.i. It either directly or through induction of other cytokines such as IL-6 (over-expressed on days 4 and 7) and TNF-α (over-expressed on day 7) promotes development of liver inflammation by increasing the expression of adhesion molecules and chemotactic factors. Recruitment of inflammatory cells, induced by the injured liver, then takes place [39] as is evident by the presence of inflammatory cell infiltrations (Figs 4 and 5).

The beta chemokines primarily have chemotactic activities for mononuclear cells; the prototypes of this group are MCP-1 and MIP-1α, both of which can induce monocyte and lymphocyte chemoattractions [40]. MCP-1 in our study showed significant increases on days 4 and 7 as well as week 2 p.i. IL-1 and TNF-α are both potent inducers of MCP-1 [41]. Although the mechanism of action of MCP-1 in the liver inflammatory process is unclear, this chemokine may directly cause impairment of hepatocyte proliferation [42]. It also recruits and activates monocytes/macrophages into the injured tissues [43]. MCP-1 is intimately involved in stimulation of the inflammatory infiltrates, and might also have immunomodulatory effects, by enhancing the expression of adhesion molecules in monocytes and promoting the synthesis of pro-inflammatory cytokine synthesis, thus intensifying the inflammation of liver tissue [44].

TGF-β is a multifunctional cytokine with key roles in development, immunity, carcinogenesis and wound healing. TGF-β represents an important link between immune cells and fibrogenic cells across organs [45]. The majority of TGF-β is produced by immune cells, including hepatic macrophages, and directly promotes fibrogenesis in myofibroblasts [38]. These elevated levels of TGF-β have been suggested to inhibit the proliferation of hepatocytes and stellate cells, acting as an inducer of apoptosis and a negative feedback mechanism [46,47]. TGF-β triggers structural abnormalities in the vasculature leading to perivascular amyloidogenesis and microvascular degeneration [48]. These effects of TGF-β explain our results of amyloid deposition around the portal vein during *T. spiralis* infection in rats (Fig. 5) and increased hepatic apoptosis associated with increased expression of TGF-β (Fig. 6).

It is worth mentioning that the accumulation of inflammatory cells in hepatic tissue during *T. spiralis* infection is crucial for the elimination of invading organisms, but overwhelming activation of these cells may amplify liver damage [38].

It is known that chronic helminth infections are often associated with polarized Th2 responses with predominantly IL-4 and IL-10 responses. IL-4 together with IL-13 promotes the expulsion of nematodes from the intestine by evoking mastocytosis, eosinophilia, intestinal muscle hypercontractility, goblet cell hyperplasia and mucous secretion [49]. IL-4 also participates in tissue repair and remodelling and controls Th1 responses and worm expulsion via alternative activation of macrophages [50]. Thus, elevated expression of hepatic IL-4 during *T. spiralis* infection might have an anti-inflammatory effect against hepatic inflammation and explains the hepatic eosinophilia that was associated with the infection (Figs 4 and 5). Notably, IL-10 has a pivotal role in regulating inflammation in the liver during *T. spiralis* infection in mice. This is evidenced by hepatic necrosis in IL-10 knock-out mice [51]; therefore, the absence of hepatic IL-10 expression up to week 5 p.i. with *T. spiralis* in rats might explain the inflammatory changes that occurred in the liver. Interestingly, there is a significant up-regulation of IL-1 mRNA in the liver of *T. spiralis*-infected rats on week 7 p.i. This was associated with encapsulation of muscle larvae and induced anti-inflammatory responses which occurred at 30–50 days p.i. [52]. It is interesting that hepatic IL-10 expression was down-regulated significantly on week 9 p.i. This observation is easily understood in the context of reduced inflammatory process after complete encapsulation of muscle larvae. Both IL-4 and IL-10 may act as anti-inflammatory mediators against necroinflammatory lesions and as an eosinophilic effector mechanism inducing liver lesions [53].

Conclusion

In this work, we provide new information about the role of the immune response mounted during infection with *T. spiralis* in male Wistar rats in induction of hepatic inflammation and subsequent decrease in serum PON1 and BuChE activities. Future work will be aimed at determining the nature of the immune response in the liver itself and the relationship between intestinal immune cells and the liver during infection.

Acknowledgements

We are grateful to the staff of the Laboratory of Veterinary Parasitic Diseases, Department of Veterinary Sciences, Faculty of Agriculture, University of Miyazaki for their valuable support. This study was supported by JSPS KAKENHI Grant Number 26450405 and in part by the Project for Zoonoses Education and Research, University of Miyazaki. One of the authors, Ayman Samir Farid, received financial support from the Scientific Research Fund, Benha University, Egypt.

Conflict of interest

The authors declare that there is no conflict of interest to disclose for this study.

Author contributions

Conceived and designed the experiments: ASF and YH. Performed the experiments: ASF, EM, SM and NN. Analysed the data: ASF and YH. Wrote the paper: ASF and YH.

Address

Department of Clinical Pathology, Faculty of Veterinary Medicine, Benha University, Moshtohor, Toukh 13736, Qalyubia, Egypt (A. S. Farid); Laboratory of Veterinary Parasitic Diseases, Interdisciplinary Graduate School of Medicine and Veterinary Medicine, University of Miyazaki, 1–1 Gakuen-Kibanadai-Nishi, Miyazaki, Miyazaki 889–2192, Japan (E. M. Fath, S. Mido, N. Nonaka, Y. Horii); Center for Animal Disease Control, University of Miyazaki, Gakuen-Kibanadai-Nishi 1-1, Miyazaki 889-2192, Japan (N. Nonaka, Y. Horii).

Correspondence to: Yoichiro Horii, Laboratory of Veterinary Parasitic Diseases, Interdisciplinary Graduate School of Medicine and Veterinary Medicine, Center for Animal Disease Control, University of Miyazaki, 1–1 Gakuen-Kibanadai-Nishi, Miyazaki, Miyazaki 889–2192, Japan. Tel.: +81 973 22 6509; fax: +81 973 22 1242; e-mail: horii@cc.miyazaki-u.ac.jp

Received 26 June 2016; accepted 16 January 2017

References

1 Bowen DG, McCaughan GW, Bertolino P. Intrahepatic immunity: a tale of two sites? *Trends Immunol* 2005;**26**:512–7.
2 Racanelli V, Rehermann B. The liver as an immunological organ. *Hepatology* 2006;**43**(2 Suppl 1):S54–62.
3 Maier M, Tappe D, Topfer C, Rosenwald A, Gassel HJ, Timm S. Nematode infection of the liver mimicking metastasis of malignant melanoma. *Liver Int* 2006;**26**:742–5.
4 Douglas DB, Beiting DP, Loftus JP, Appleton JA, Bliss SK. Combinatorial effects of interleukin 10 and interleukin 4 determine the progression of hepatic inflammation following murine enteric parasitic infection. *Hepatology* 2010;**51**:2162–71.
5 Gabay C, Kushner I. Acute-phase proteins and other systemic responses to inflammation. *N Engl J Med* 1999;**340**:448–54.
6 Feingold KR, Memon RA, Moser AH, Grunfeld C. Paraoxonase activity in the serum and hepatic mRNA levels decrease during the acute phase response. *Atherosclerosis* 1998;**139**:307–15.
7 Aviram M, Hardak E, Vaya J, Mahmood S, Milo S, Hoffman A *et al.* Human serum paraoxonases (PON1) Q and R selectively decrease lipid peroxides in human coronary and carotid atherosclerotic lesions: PON1 esterase and peroxidase-like activities. *Circulation* 2000;**101**:2510–7.
8 Aviram M, Rosenblat M, Bisgaier CL, Newton RS, Primo-Parmo SL, La Du BN. Paraoxonase inhibits high-density lipoprotein oxidation and preserves its functions. A possible peroxidative role for paraoxonase. *J Clin Investig* 1998;**101**:1581–90.
9 Rosenblat M, Vaya J, Shih D, Aviram M. Paraoxonase 1 (PON1) enhances HDL-mediated macrophage cholesterol efflux via the ABCA1 transporter in association with increased HDL binding to the cells: a possible role for lysophosphatidylcholine. *Atherosclerosis* 2005;**179**:69–77.
10 Aviram M, Rosenblat M. Paraoxonases 1, 2, and 3, oxidative stress, and macrophage foam cell formation during atherosclerosis development. *Free Radic Biol Med* 2004;**37**:1304–16.
11 Mackness B, Mackness M. Anti-inflammatory properties of paraoxonase-1 in atherosclerosis. *Adv Exp Med Biol* 2010;**660**:143–51.
12 Farid AS, Horii Y. Modulation of paraoxonases during infectious diseases and its potential impact on atherosclerosis. *Lipids Health Dis* 2012;**11**:92.
13 Tvarijonaviciute A, Caldin M, Martinez-Subiela S, Tecles F, Pastor J, Ceron JJ. Serum paraoxonase 1 and butyrylcholinesterase in dogs with hyperadrenocorticism. *Vet J* 2015;**203**:262–3.
14 Iwasaki T, Yoneda M, Nakajima A, Terauchi Y. Serum butyrylcholinesterase is strongly associated with adiposity, the serum lipid profile and insulin resistance. *Intern Med* 2007;**46**:1633–9.
15 Darvesh S, Hopkins DA, Geula C. Neurobiology of butyrylcholinesterase. *Nat Rev Neurosci* 2003;**4**:131–8.
16 Mido S, Fath EM, Farid AS, Nonaka N, Oku Y, Horii Y. *Trichinella spiralis*: infection changes serum paraoxonase-1 levels, lipid profile, and oxidative status in rats. *Exp Parasitol* 2012;**131**:190–4.
17 Farid AS, Mido S, Linh BK, Hayashi T, Horii Y. An atherogenic lipid profile with low serum paraoxonase-1 activity during nematode infection in rats. *Eur J Clin Invest* 2010;**40**:984–93.
18 Farid AS, Shimohira T, Kobayashi I, Sawada J, Horii Y. Intestinally implanted *Nippostrongylus brasiliensis* adult worms decrease serum paraoxonase-1 activity in rats. *Parasitol Int* 2009;**58**:178–83.
19 Farid AS, Horii Y. *Nippostrongylus brasiliensis*: infection decreases plasma butyrylcholinesterase activity in rats. *Exp Parasitol* 2009;**122**:162–4.
20 Kang SA, Park MK, Cho MK, Park SK, Jang MS, Yang BG *et al.* Parasitic nematode-induced $CD4^{+}Foxp3^{+}$T cells can ameliorate allergic airway inflammation. *PLoS Negl Trop Dis* 2014;**8**:e3410.
21 Yu YR, Deng MJ, Lu WW, Jia MZ, Wu W, Qi YF. Systemic cytokine profiles and splenic toll-like receptor expression during *Trichinella spiralis* infection. *Exp Parasitol* 2013;**134**:92–101.
22 Crum ED, Despommier DD, McGregor DD. Immunity to *Trichinella spiralis*. I. Transfer of resistance by two classes of lymphocytes. *Immunology* 1977;**33**:787–95.
23 Aviram M, Rosenblat M. Paraoxonases (PON1, PON2, PON3) analyses *in vitro* and *in vivo* in relation to cardiovascular diseases. *Methods Mol Biol* 2008;**477**:259–76.
24 Schmittgen TD, Livak KJ. Analyzing real-time PCR data by the comparative C(T) method. *Nat Protoc* 2008;**3**:1101–8.
25 Barut Ş, Ünlü YA, Karaoğlan A, Tunçdemir M, Dağistanli FK, Öztürk M *et al.* The neuroprotective effects of z-DEVD. fmk, a caspase-3 inhibitor, on traumatic spinal cord injury in rats. *Surg Neurol* 2005;**64**:213–20.
26 Parker GA, Picut CA. Liver immunobiology. *Toxicol Pathol* 2005;**33**:52–62.
27 McDermott JR, Leslie FC, D'Amato M, Thompson DG, Grencis RK, McLaughlin JT. Immune control of food intake: enteroendocrine cells are regulated by CD4 + T lymphocytes during small intestinal inflammation. *Gut* 2006;**55**:492–7.
28 Lal S, McLaughlin J, Barlow J, D'Amato M, Giacovelli G, Varro A *et al.* Cholecystokinin pathways modulate sensations induced by gastric distension in humans. *Am J Physiol Gastrointest Liver Physiol* 2004;**287**:G72–9.
29 Mackness MI, Mackness B, Durrington PN, Connelly PW, Hegele RA. Paraoxonase: biochemistry, genetics and relationship to plasma lipoproteins. *Curr Opin Lipidol* 1996;**7**:69–76.

30 Thomas-Moya E, Gianotti M, Proenza AM, Llado I. Paraoxonase 1 response to a high-fat diet: gender differences in the factors involved. *Mol Med* 2007;**13**:203–9.
31 Kumon Y, Suehiro T, Ikeda Y, Hashimoto K. Human paraoxonase-1 gene expression by HepG2 cells is downregulated by interleukin-1β and tumor necrosis factor-α, but is upregulated by interleukin-6. *Life Sci* 2003;**73**:2807–15.
32 Han CY, Chiba T, Campbell JS, Fausto N, Chaisson M, Orasanu G *et al*. Reciprocal and coordinate regulation of serum amyloid A versus apolipoprotein A-I and paraoxonase-1 by inflammation in murine hepatocytes. *Arterioscler Thromb Vasc Biol* 2006;**26**:1806–13.
33 Jakab SS. *Clinical Hepatology—Principles and Practice of Hepatobiliary Diseases*. Philadelphia, PA: LWW; 2010.
34 McNeil KS, Knox DP, Proudfoot L. Anti-inflammatory responses and oxidative stress in *Nippostrongylus brasiliensis*-induced pulmonary inflammation. *Parasite Immunol* 2002;**24**:15–22.
35 Smith NC, Ovington KS, Bryant C. Free radical generation and the course of primary infection with *Nippostrongylus brasiliensis* in congenitally athymic (nude) rats. *Parasite Immunol* 1991;**13**:571–81.
36 Li WF, Costa LG, Furlong CE. Serum paraoxonase status: a major factor in determining resistance to organophosphates. *J Toxicol Environ Health* 1993;**40**:337–46.
37 Lucic Vrdoljak A, Bradamante V, Radic B, Peraica M, Fuchs R, Reiner Z. Butyrylcholinesterase activity and plasma lipids in dexamethasone treated rats. *Acta Pharm* 2005;**55**:177–85.
38 Seki E, Schwabe RF. Hepatic inflammation and fibrosis: functional links and key pathways. *Hepatology* 2015;**61**:1066–79.
39 Kamari Y, Shaish A, Vax E, Shemesh S, Kandel-Kfir M, Arbel Y *et al*. Lack of interleukin-1alpha or interleukin-1beta inhibits transformation of steatosis to steatohepatitis and liver fibrosis in hypercholesterolemic mice. *J Hepatol* 2011;**55**:1086–94.
40 Fisher NC, Neil DA, Williams A, Adams DH. Serum concentrations and peripheral secretion of the beta chemokines monocyte chemoattractant protein 1 and macrophage inflammatory protein 1alpha in alcoholic liver disease. *Gut* 1999;**45**:416–20.
41 Khoruts A, Stahnke L, McClain CJ, Logan G, Allen JI. Circulating tumor necrosis factor, interleukin-1 and interleukin-6 concentrations in chronic alcoholic patients. *Hepatology* 1991;**13**:267–76.
42 Leifeld L, Dumoulin FL, Purr I, Janberg K, Trautwein C, Wolff M *et al*. Early up-regulation of chemokine expression in fulminant hepatic failure. *J Pathol* 2003;**199**:335–44.
43 Simpson KJ, Henderson NC, Bone-Larson CL, Lukacs NW, Hogaboam CM, Kunkel SL. Chemokines in the pathogenesis of liver disease: so many players with poorly defined roles. *Clin Sci* 2003;**104**:47–63.
44 Jiang Y, Beller DI, Frendl G, Graves DT. Monocyte chemoattractant protein-1 regulates adhesion molecule expression and cytokine production in human monocytes. *J Immunol* 1992;**148**:2423–8.
45 Liu X, Hu H, Yin JQ. Therapeutic strategies against TGF-beta signaling pathway in hepatic fibrosis. *Liver Int* 2006;**26**:8–22.
46 Dooley S, Delvoux B, Lahme B, Mangasser-Stephan K, Gressner AM. Modulation of transforming growth factor beta response and signaling during transdifferentiation of rat hepatic stellate cells to myofibroblasts. *Hepatology* 2000;**31**:1094–106.
47 McMahon JB, Richards WL, del Campo AA, Song M-KH, Thorgeirsson SS. Differential effects of transforming growth factor-β on proliferation of normal and malignant rat liver epithelial cells in culture. *Cancer Res* 1986;**46**:4665–71.
48 Burton T, Liang B, Dibrov A, Amara F. Transcriptional activation and increase in expression of Alzheimer's β-amyloid precursor protein gene is mediated by TGF-β in normal human astrocytes. *Biochem Biophys Res Commun* 2002;**295**:702–12.
49 Liu Z, Liu Q, Pesce J, Anthony RM, Lamb E, Whitmire J *et al*. Requirements for the development of IL-4-producing T cells during intestinal nematode infections: what it takes to make a Th2 cell in vivo. *Immunol Rev* 2004;**201**:57–74.
50 Kreider T, Anthony RM, Urban JF Jr, Gause WC. Alternatively activated macrophages in helminth infections. *Curr Opin Immunol* 2007;**19**:448–53.
51 Bliss SK, Alcaraz A, Appleton JA. IL-10 prevents liver necrosis during murine infection with *Trichinella spiralis*. *J Immunol* 2003;**171**:3142–7.
52 Walls RS, Hersey P, Quie PG. Macrophage-eosinophil interactions in the inflammatory response to *Trichinella spiralis*. *Blood* 1974;**44**:131–6.
53 dos Santos DC, da Silva Gomes Martinho JM, Pacheco-Moreira LF, Carvalho Viana de Araujo C, Caroli-Bottino A, Pannain VL *et al*. Eosinophils involved in fulminant hepatic failure are associated with high interleukin-6 expression and absence of interleukin-5 in liver and peripheral blood. *Liver Int* 2009;**29**:544–51.